JOURNAL OF GEOPHYSICAL RESEARCH, VOL. 114, A07212, doi:10.1029/2009JA014289, 2009

Auroral footprint of Ganymede

Denis Grodent,[1] Bertrand Bonfond,[1] Aikaterini Radioti,[1] Jean-Claude Gérard,[1] Xianzhe Jia,[2] Jonathan D. Nichols,[3] and John T. Clarke[4]

Received 24 March 2009; revised 5 May 2009; accepted 8 May 2009; published 10 July 2009.

[1] The interaction of Ganymede with Jupiter's fast rotating magnetospheric plasma gives rise to a current system producing an auroral footprint in Jupiter's ionosphere, usually referred to as the Ganymede footprint. Based on an analysis of ultraviolet images obtained with the Hubble Space Telescope, we demonstrate that the auroral footprint surface matches a circular region in Ganymede's orbital plane having a diameter of 8–20 R_G. Temporal analysis of the auroral power of Ganymede's footprint reveals variations of different timescales: (1) a 5-hour timescale associated with the periodic flapping of Jupiter's plasma sheet over Ganymede, (2) a 10–40 minute timescale possibly associated with energetic magnetospheric events, such as plasma injections, and (3) a 100-s timescale corresponding to quasiperiodic fluctuations, which might relate to bursty reconnections on Ganymede's magnetopause and/or to the recurrent presence of acceleration structures above Jupiter's atmosphere. These three temporal components produce an auroral power emitted at Ganymede's footprint of the order of ~0.2 to ~1.5 GW.

Citation: Grodent, D., B. Bonfond, A. Radioti, J.-C. Gérard, X. Jia, J. D. Nichols, and J. T. Clarke (2009), Auroral footprint of Ganymede, *J. Geophys. Res.*, *114*, A07212, doi:10.1029/2009JA014289.

1. Introduction

[2] Ganymede is Jupiter's third most distant Galilean moon. It is embedded in the Jovian plasma rapidly rotating around the planet. At Ganymede's orbital radius ~15 R_J (1 R_J = 71492 km), the plasma flow is ~14 times faster than Ganymede's orbital velocity, assuming that the convective plasma flow speed is 80% of the rigid corotation speed [*Khurana et al.*, 2004]. A key property of Ganymede is its intrinsic magnetic field [*Kivelson et al.*, 1996]. The permanent dipole is almost aligned with the moon's spin axis and its equatorial surface strength is ~7 times the ambient planetary field, strong enough to stand off the flow above the surface and form a small magnetosphere within Jupiter's magnetosphere. As a result, most of the Jovian magnetospheric plasma is diverted around a roughly cylindrical region defining Ganymede's magnetopause with a standoff distance of order of 2 R_G (1 R_G = Ganymede's radius = 2634 km) measured from the moon's center. For other satellites, the satellite itself is considered as the obstacle in the flow. However, in the case of Ganymede the obstacle is its magnetosphere. The first order interaction between Ganymede's magnetosphere and Jupiter's magnetic field is not very different from the interaction between a rotating planetary field and a conducting body such as Io. The major difference arises because, as a result of Ganymede's dipole orientation, Jupiter's field lines reconnect with Ganymede's field lines which are attached to its polar caps. These newly reconnected flux tubes carrying the Jovian plasma are decelerated to Ganymede's velocity and cause the field lines to bend. This perturbation propagates along the field lines and forms two Alfvén wings extending into the northern and southern ionosphere of Jupiter. These wings bound field aligned currents connecting Ganymede's magnetosphere to Jupiter's ionosphere. Unidirectional (toward Ganymede's surface) electron beams have been observed by Galileo in Ganymede's magnetosphere [*Williams*, 2004]. However, they were detected on Ganymede's closed magnetic field lines and therefore these beams do not participate to the current system responsible for Ganymede's auroral footprint. *Jia et al.* [2008] developed a three-dimensional global magnetohydrodynamic model to simulate with high spatial resolution the interaction between the Jovian plasma and Ganymede's magnetosphere. These simulations are constrained with in situ measurements obtained during Galileo's six close encounters of Ganymede. They provide a consistent description of the interaction region as well as reliable estimate of the total current carried by the Alfvén wings. Among other results, *Jia et al.* [2008] suggest that the Alfvén wing currents close not only through the moon and its ionosphere, but also through the magnetopause and tail current sheets. They estimate that 50% of the total current closes through Ganymede and its ionosphere, 35% closes on the downstream side of its magnetotail, and 15% closes near the equator via perpendicular currents along the upstream magnetopause of Ganymede. Accordingly, the interaction region extends far downstream of Ganymede, at distances which might be larger than 10 R_G.

[1]Institut d'Astrophysique et de Géophysique, Laboratory for Planetary and Atmospheric Physics, Université de Liège, Liège, Belgium.
[2]Institute of Geophysics and Planetary Physics, University of California, Los Angeles, California, USA.
[3]Department of Physics and Astronomy, University of Leicester, Leicester, UK.
[4]Center for Space Physics, Boston University, Boston, Massachusetts, USA.

0148-0227/09/2009JA014289$09.00

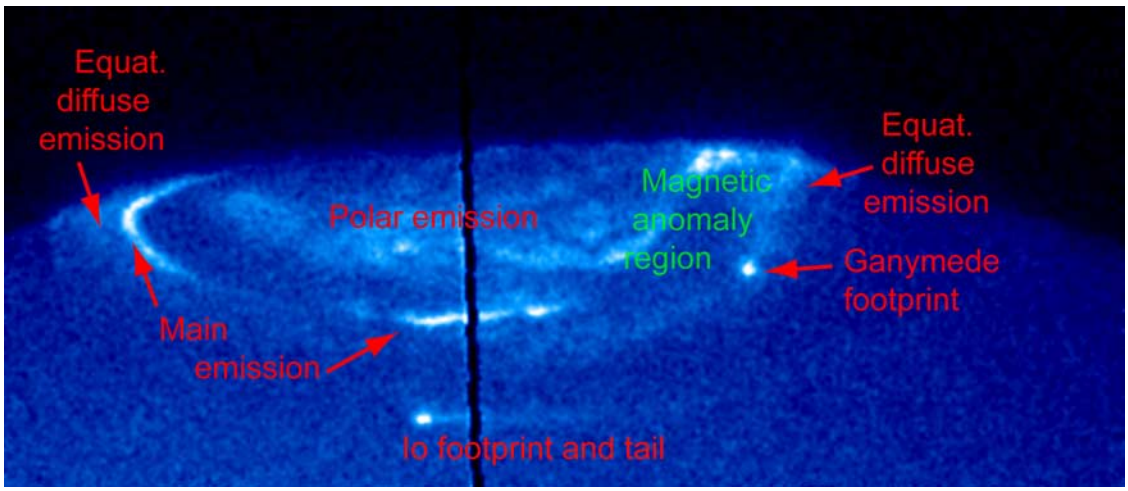

Figure 1. Raw HST image (zoom) of Jupiter's northern auroral region displaying the ultraviolet footprint of Ganymede in the anomaly region. Other auroral features such as the polar emission and the footprint of Io and its tail are also highlighted. The main emission forms a partial narrow arc (bottom) near noon and (left) in the dawn sector. It is not defined in (right) the magnetic anomaly region where equatorward diffuse auroral emission contributes to the background affecting the GFP brightness. The vertical black column corresponds to the region occulted by the detector's repelling wire. The image was obtained with HST/ACS/SBC with the F125LP filter on 2 March 2007 during the GO-10862 HST campaign. The central meridian longitude is 145° (S3), and the exposure time is 100 s.

[3] The Alfvén currents mediating the interaction between Ganymede's magnetosphere and Jupiter's magnetosphere close in the Jovian ionosphere where they produce an auroral signature recognized as the Ganymede footprint (GFP). Auroral ultraviolet (UV) emissions follow collisions of downward (planetward) electrons (upward current) with the main constituents of the Jovian upper atmosphere; H_2, giving rise to the Lyman and Werner emission bands and H, producing the strong Lyman-α line. So far, very little has been written about the GFP [*Clarke et al.*, 2002] mainly because of its relatively low brightness, compared to the main components of the Jovian aurora: the main oval and the Io footprint [e.g., *Grodent et al.*, 2003a, 2003b], and because of its proximity to the main auroral emission (the main oval) which made it unfeasible to detect with the first generation UV cameras onboard the Hubble Space Telescope (HST). The advent of the HST/STIS imaging spectrograph and later the HST/ACS camera brought the spatial resolution and sensitivity that were necessary to provide images revealing the auroral footprint of Ganymede (and Europa). The GFP is now detected in HST images on a routine basis, and a recent large HST campaign provided many ACS images displaying the GFP (Figure 1). Numerous locations made it possible to build a closed footpath around the magnetic north pole [*Grodent et al.*, 2008a]. This Ganymede contour provides a convenient absolute landmark for locating the magnetospheric source of auroral features appearing in its vicinity. It is also useful to constrain models of the Jovian magnetic field such as in the recent analysis of *Grodent et al.* [2008a] who used the auroral footpaths of Ganymede, Europa and Io to provide evidence for the presence of a magnetic anomaly near the surface of the Jovian northern hemisphere. *Khurana* [2001] and *Bunce et al.* [2002] suggested that near the orbit of Ganymede the radial component of the current sheet field, which is stretching the Jovian field lines away from Jupiter, is ranging from 30 to 40 nT, depending on local time. This range is comparable to the radial component of the internal field, which at this distance is mainly dipolar. The magnetic field lines crossing Ganymede's orbit are thus significantly affected by the external field produced by the current sheet. Based on HST observations, *Grodent et al.* [2008b] suggested that the latitude of the GFP may indeed change by a couple of degrees in response to large variations (factor of 2 or 3) of the current flowing in the current sheet. The latitudinal change of the auroral emission compared to Ganymede's reference contour may then be used as a proxy for estimating the current sheet parameters.

[4] It was originally thought that the polar caps of Ganymede would be completely filled with auroral emission originating from the direct precipitation of Jovian magnetospheric plasma along open magnetic field lines. However, *Feldman et al.* [2000] showed that the oxygen auroral emissions at Ganymede appear at the foot of Ganymede's high latitude closed field lines, whereas the Alfvén wing connecting Ganymede to Jupiter and the GFP travels along open field lines. Therefore the electromagnetic link between the emissions at Jupiter and at Ganymede is not straightforward and has not been addressed in this study. The only temporal variation of Ganymede's auroral brightness reported to date [*Feldman et al.*, 2000] is characterized by a timescale corresponding to 1 HST orbit (96 min), observed over 4 contiguous HST orbits. These variations were tentatively attributed to changing Jovian plasma environment at Ganymede.

[5] In the present study, the case of the GFP is investigated with upgraded versions of the tools that we have developed for the Io footprint (IFP). The electromagnetic interaction between Io and the Jovian plasma contained in the Io torus leads to a complex auroral pattern in the

ionosphere of Jupiter. Variations of the footprint emission number, location and brightness have been shown to be related to Io's position in the Io torus, with brighter emissions when Io is near the center of the torus, where the plasma is denser, suggesting that long timescale (10 h) brightness variations are primarily controlled by the strength of the moon-Io torus plasma interaction [*Gérard et al.*, 2006]. The detailed structure of the IFP also appears to be consistent with Alfvén wave reflections in the torus combined with the acceleration of transhemispheric electron beams at the footprint [*Bonfond et al.*, 2008]. In addition, *Bonfond et al.* [2007] showed strong brightness variations of the main auroral footprint emission with typical growth time of 1 min, implying that electron acceleration processes occurring between the torus and Jupiter are also influencing the IFP brightness.

2. Observations

[6] We consider a total of 753 HST images of the Northern (678 images) and Southern (75 images) auroral regions of Jupiter in which the footprint of Ganymede is visible. Most of the images (547) were taken during HST program GO-10862 obtained during a 5-month observation campaign starting in February 2007. The example image displayed in Figure 1 was extracted from this data set. It illustrates different auroral features which may be observed in the northern hemisphere. We complete this large HST campaign with two more modest data sets; the GO-10140 HST program executed between April and May 2005 and the GO-10507 HST program achieved between February and April 2006. They were all obtained with the photon-counting Multi-Anode Microchannel Array (MAMA) of the Solar Blind Channel (SBC) on the Advanced Camera for Surveys (ACS). These programs consist of ultraviolet images captured with the F125LP and F115LP filters. The F125LP long-pass filter is sensitive to the H_2 far UV Lyman and Werner bands but rejects emissions shortward of 125 nm, therefore mostly excluding the H Lyman-α line, contrary to the case of the F115LP filter. The average plate scale of 0.032 arcs per pixel of ACS provides a field of view of 35×31 arcsec^2 which is comparable to Jupiter's apparent equatorial diameter of $\sim$40 arcsec. In addition to these ACS images, we take into account seven time-tagged sequences of Jupiter's Northern auroral emissions obtained with the Space Telescope Imaging Spectrograph (STIS) during HST programs GO-7308 (July 1998), GO-8171 (September 1999), GO-8657 (December 2000–January 2001), and GO-9685 (February 2003). In order to reach a satisfactory tradeoff between time resolution and signal-to-noise ratio, we build 10-second exposure images from the time-tagged events lists. All STIS/MAMA time tagged sequences were obtained with the SrF2 filter, similar to the F125LP ACS filter. The STIS 25×25 arcsec^2 field of view is slightly smaller than ACS. In both cases, approximately one quarter of Jupiter's planetary disk fits in the field of view and the planet center is never included in the images. Accordingly, we have used the fully automatic numerical method described by *Bonfond et al.* [2009] to estimate Jupiter's center position outside the field of view and derive the jovicentric latitude and System III (S3) longitude of the central location of Ganymede's auroral footprint. All images were preprocessed with standard calibration pipelines for dark count subtraction, flat-fielding and geometrical distortion correction.

3. Ganymede Footprint Size and Background Selection

[7] The auroral footprint of Ganymede is selected manually on each image since automatic procedures generally fail to discriminate the GFP from the rest of the auroral emission. For the STIS and ACS images, we first locate the center position of the footprint emission and then define the semimajor and semiminor axis of a tilted ellipse fitting the boundary of the footprint emission. A second ellipse is defined near the auroral footprint emission and is used to evaluate the average local auroral background (BKG) mainly owing to diffuse emission (Figure 1) equatorward of the main emission [*Radioti et al.*, 2009]. The useful portion of one HST orbit is usually of the order of 45 minutes. During this time the lower latitude auroral morphology does not vary much [*Nichols et al.*, 2009] so that it is reasonable to assume that the size of both ellipses is approximately constant during one orbit while the GFP center position smoothly changes with the 20° to 30° rotation of the S3 coordinate system. The case of the shorter STIS time-tagged sequences is similar, the only difference being that the GFP and BKG ellipse characteristics are defined only once for all subimages.

[8] The GFP ellipse covers $\sim$43 pixels^2 on the images with a standard deviation of 34% over the data set. This area is $\sim$6 times larger than the area subtended by the detector's point spread function. Accordingly, the average area of the GFP ellipse is approximately 0.04 arcsec^2 which corresponds to $\sim 5 \times 10^5$ km^2 on Jupiter. Magnetic flux conservation along the flux tube threading the GFP implies that the magnetic field $\times$ cross section product is invariable and provides an estimate of the corresponding region area in the equatorial plane. Considering the variability of the measured footprint area (the 34% standard deviation), the equatorial region giving rise to the UV GFP is characterized by a circular cross section having a radius ranging from 10 to 30 R_G. If one takes Ganymede's internal field into account, which is about 7 times larger than the ambient field, then an additional focusing effect applies near Ganymede (Figure 2) and the radius range drops to approximately 4 to 10 R_G. This information constrains the size of the interaction region between the Jovian plasma flowing in the current sheet and Ganymede and will be discussed below in view of the recent study of *Jia et al.* [2008].

4. Temporal Analysis

[9] We observe emitted power variations over three distinct timescales, ranging from five hours to hundreds of seconds. These temporal variations are conveniently expressed in terms of the orbital longitude of Ganymede in S3. In that regard, we note that Ganymede's S3 orbital longitude increases by 1 degree in 105.33 s. The advantages of S3 longitude is that it provides additional information on the location of Ganymede with respect to the current sheet and it makes it possible to accumulate data points obtained at different times. It should be kept in mind that the

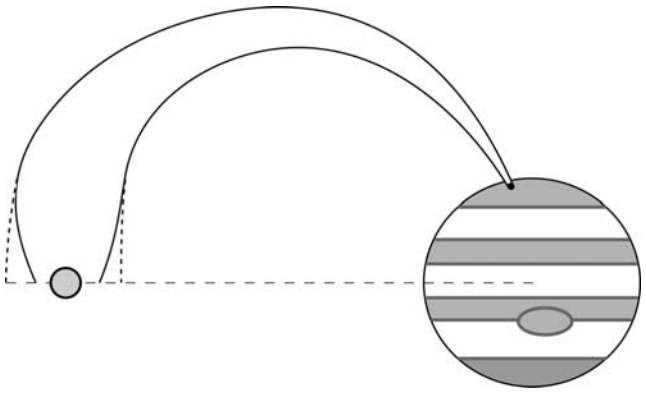

Figure 2. Illustration of (right) the magnetic field lines focusing toward the surface of Jupiter and (left) the additional focusing, stemming from Ganymede's internal field, which squeezes the field lines toward Ganymede. The dashed lines represent the case where Ganymede's internal field is not taken into account and for which the additional focusing does not apply. After correction for both effects, the area subtended by the auroral footprint on Jupiter matches the area of a circular surface on Ganymede's orbital plane with a diameter of 8 to 20 R_G. The sketch is not to scale and the southern portion of the magnetic flux tube is not represented for clarity.

traveltime of an Alfvén wave from Ganymede to Jupiter's ionosphere is mainly controlled by the time spent to cross the current sheet. If one assumes an Alfvén wave crossing half of the current sheet thickness ($\sim$2 R_J) at an average velocity of 200 km s^{-1} then the traveltime is on the order of 12 min. Outside the current sheet, the Alfvén wave reaches relativistic speed and the traveltime is on the order of several seconds. This travel imparts a delay of a couple of tens of minutes between a fluctuation of the interaction near Ganymede and its auroral signature on Jupiter.

4.1. The 5-Hour Timescale

[10] The first, longest, timescale is comparable to one half of Jupiter's magnetic field rotation period, i.e. approximately five hours. Figure 3 shows that Ganymede's footprint emitted power as a function of its orbital longitude varies from $\sim$0.2 GW to $\sim$1.5 GW. The 65 images where the auroral footprint cannot be unambiguously discriminated from the background auroral emission or where the footprint lies above the planetary limb were not included in the analysis. A clear sinusoidal trend appears in the plot. It is highlighted with a continuous curve resulting from a Fourier series fit with two harmonics. The solid section of the curve fits the 566 data points corresponding to unambiguous cases in the northern hemisphere (stars and plus symbols) and the dashed section is largely influenced by 47 northern cases (diamonds) where the GFP is well defined but for which the surrounding auroral background is large and/or differs significantly between the region ahead or behind of the footprint. In such cases we subtract the lowest background value and the resulting GFP power is likely overestimated by up to 30%. However, this latter uncertainty is not sufficient to change the general trend of the curve. This trend is further confirmed by the 75 data points in the southern hemisphere (triangles) and to some extent by the 131 additional points obtained during previous ACS campaigns (crosses), 18 of these points (S3 longitude between $\sim$260° and 290°) were observed when the GFP was very close to the limb and might not have been properly corrected for BKG emission, they also contribute to the dashed section of the trend displayed in Figure 3. The error bars on the points leading to the solid part of the Fourier curve are equal to ± the Poisson noise, i.e. ± the square root

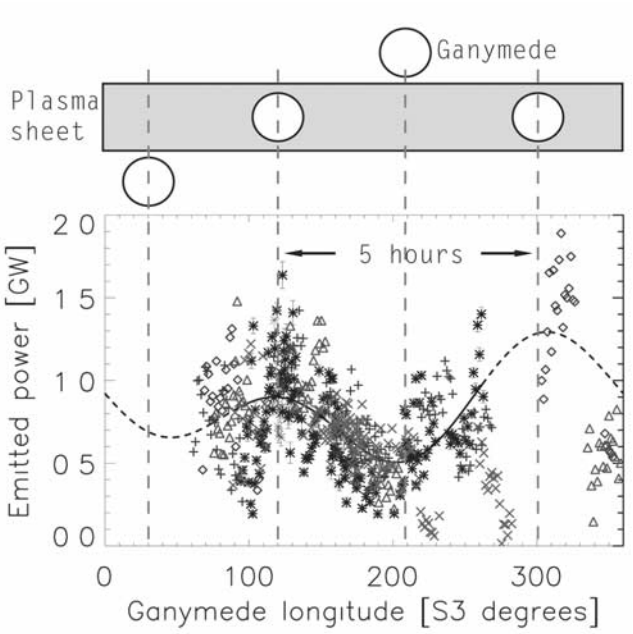

Figure 3. Illustration of the 5-hour timescale. The emitted power of Ganymede's auroral footprint above the BKG emission is plotted as a function of Ganymede's orbital longitude in S3 degrees and, consistently, as a function of Ganymede's latitude in Jupiter's plasma sheet (the top sketch is just a visual aid). Most of the data points were collected in the HST/ACS database obtained during a 5-month HST observation campaign in 2007. "Star" and "plus" symbols correspond to 566 images unambiguously showing the GFP in the northern hemisphere. The 47 "diamonds" refer to acceptable northern cases where the GFP is well defined but for which the BKG is relatively large and might lead to a 30% overestimation of the emitted power. 75 triangles represent data points which were collected in the Southern Hemisphere. Crosses point to 131 images obtained during previous HST/ACS campaigns in 2005 and 2006. The continuous curve was obtained with a Fourier series fit with two harmonics period. It highlights the sinusoidal shape formed by the data points. The solid section of the curve fits 566 unambiguous data points (stars and plus symbols), and the dashed section is largely influenced by 47 footprints observed in 2007 (diamonds) and 18 cases in 2006 (crosses), which were observed very close to the limb and might be affected by the BKG subtraction method. The peak-to-peak delay corresponds to a period of $\sim$5 hours. This period and the location of the extrema suggest that the GFP emitted power is strongly modulated by the latitude of Ganymede in the plasma sheet. The observed power varies between $\sim$0.2 GW and $\sim$1.5 GW above the BKG.

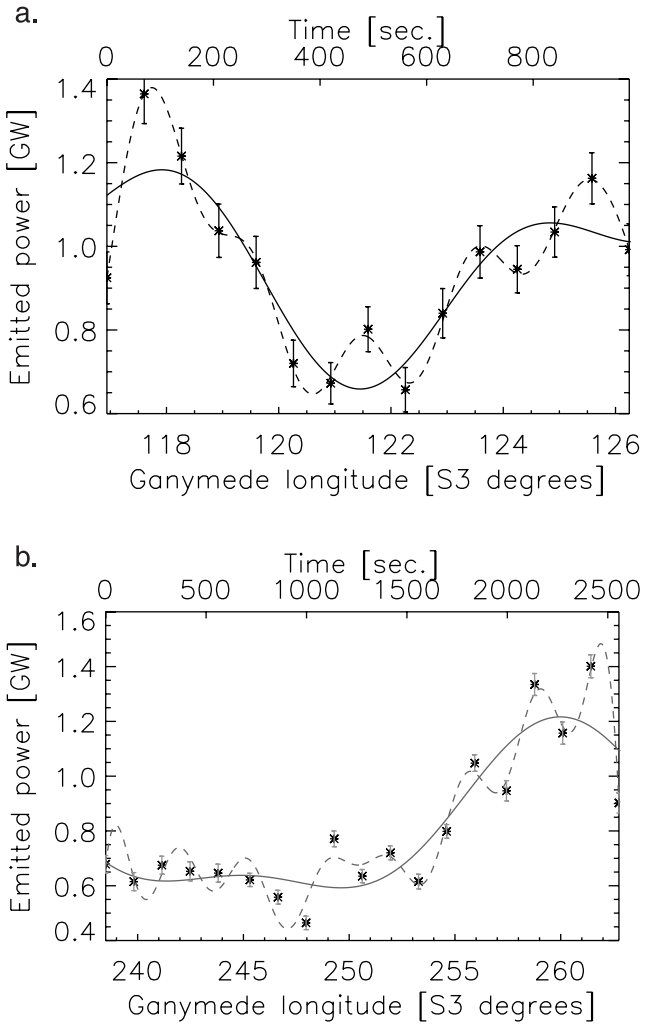

Figure 4. Illustration of the 10–40 minute timescale. The auroral power emitted at the GFP above the BKG emission is plotted as a function of the S3 orbital longitude of Ganymede for one HST orbit at the time. (a) Representative example taken from the pool of strong cases. The general trend is underlined by the solid curve representing a Fourier series fit with two harmonics while the dashed curve stands for a six-harmonic Fourier series revealing a shorter period. The error bars are determined from the Poisson noise and are about five times smaller than the amplitude of the variation. The observed data points vary between a maximum power above the BKG of 1.4 GW and a minimum value of 0.65 GW, and the average power is about 1 GW. The peak-to-peak distance is about 8° of S3 longitude which represents a time delay of approximately 14 minutes. (b) A typical variation over a wider range of longitudes. The two-harmonic Fourier curve (solid line) highlights a plateau at 0.6 GW followed by a rapid power increase to 1.4 GW. The characteristic time of the growth phase from the end of the plateau to the peak value is about 18 minutes.

of the total, background plus GFP, count number scaled to the y axis units (GW). They demonstrate that the power variation trend is too large to stem from statistical fluctuations. In addition, we have verified that it is not the background itself, which produces the observed power variations. It should also be noted that a range of S3 orbital longitudes usually combines observations obtained at different orbital phase angles, so that it might be ascertained that the global trend showing up in Figure 3 does not result from a viewing geometry effect. Hence limb brightening effects have no influence on the measured power since this power is evaluated over the whole emitting area. Since the x axis of Figure 3 spans 360° degrees and since the data points were accumulated over several years, the strong sinusoidal shape of the fitting curve may be interpreted as a periodical signal, with a peak-to-peak period of ~5 h. It suggests that the GFP emitted power is strongly modulated by a combination of Ganymede's position along its orbit and the rotation of Jupiter's magnetic field. The solid section of the fitted curve reaches a maximum value near 120° S3 longitude and drops to a minimum power at ~200°. The dashed section of the curve is less reliable but it suggests a larger maximum near 310° and a shallower minimum around 40° S3 longitude. The location of these four extrema indicates that the GFP emitted power is most likely modulated by the north-south location of Ganymede relative to the plasma sheet (see sketch on upper part of Figure 3). The plasma sheet behaves like a rigid structure near Jupiter's magnetic dipole equator inside a radial distance of ~50 R_J [*Khurana and Schwarzl*, 2005]. At Ganymede's orbit (15 R_J) the tilted current sheet approximately coincides with the expected location of the dipole magnetic equator. Accordingly, the two maxima at 120° and 310° are very close to the S3 orbital longitudes where Ganymede reaches the center of the plasma sheet while the minimum at 200° tallies with the highest position of Ganymede above (north of) the plasma sheet. Near the 40° minimum, Ganymede is located below (south of) the sheet. The plasma density varies across the sheet from a large value near the center to lower values at the boundaries. According to *Kivelson et al.* [2004], as the thick plasma sheet flutters over Ganymede, the ambient plasma density changes by a factor of ~5 around an average ion plasma density of 4 cm^{-3}. It may then be concluded that the GFP emitted power is significantly responding to the variations of the plasma sheet density interacting with Ganymede, resulting from the current sheet tilt to Ganymede's orbital plane, with a stronger plasma density giving rise to larger emitted power. It should be kept in mind that other (undetermined) mechanisms, such as those depending on periodic variation of the ambient magnetic field, could also modulate the interaction strength with a similar 5-hour period.

4.2. The 10–40 Minute Timescale

[11] The scatter of the data points along the Fourier curve in Figure 3 suggests a second timescale for the variation of the GFP emitted power. Two examples are shown in Figure 4 where we plot the power emitted by the GFP above the BKG emission as a function of the S3 orbital longitude of Ganymede for one HST orbit at the time. As for Figure 3, since Ganymede's orbital velocity is constant, the transformation from longitude to time is a constant scale factor of 105.33 s per degree. Among the 36 orbits that we considered in this analysis, 64% undeniably demonstrate a strong variation, 11% show less prominent changes, and 25% are more questionable or show no clear trend.

[12] Figure 4a shows a representative example taken from the pool of strong cases; this specific orbit was obtained with the same filter (F125LP). As a consequence, we can be sure that the observed variation is not caused by a filter change during the HST orbit. The general trend is underlined by the solid curve representing a Fourier series fit with two harmonics period. The dashed curve stands for a six harmonics Fourier series and will be discussed below. The error bars determined from the Poisson noise (see above) are about 5 times smaller than the amplitude of the variation. Most of them intercept the Fourier curve; accordingly we can ascertain that the variation is real and does not result from statistical fluctuations. The observed data points vary between a maximum power above the BKG of ~1.4 GW and a minimum value of ~0.65 GW, while the average power is ~1 GW. The peak-to-peak distance is ~8° of S3 longitude (~14 min). The case plotted in Figure 4b also shows a typical variation but over a large range of longitudes than in Figure 4a. The two-harmonic Fourier curve (solid line) highlights a plateau at 0.6 GW followed by a rapid power increase to 1.4 GW. The characteristic time of the growth phase, from the end of the plateau to the peak value is about 18 minutes. All other instances from the pool of strong variation cases (23 cases, representing 64% of the data set) display similar kinds of variations. Their characteristic time varies from 10 to 40 minutes. The amplitude of the variation is usually on the order of 50% of the power averaged over the longitude range, that is always much larger than the statistical fluctuations. The different cases are relatively well distributed within a range of S3 orbital longitudes from 90° to 270°. Within this range of viewing geometries, we do not note any apparent correlation between the amplitude and the characteristic time with the S3 longitude and, a fortiori, the S3 longitude of the ionospheric footprint, nor with the local time phase angle of Ganymede.

[13] These characteristic times are comparable to the duration of the observation sequences, accordingly it cannot be concluded that the observed power variations are periodic. However, we can ascertain that the variations are recurrent and once they occur they take place within approximately 10 to 40 minutes.

4.3. The 100-s Timescale

[14] The dashed curves appearing in Figures 4a and 4b represent a 6 and 8 harmonics Fourier series, respectively, closely fitting the data points. They draw our attention to a third power variation, which is clearly periodic with a peak-to-peak period close to 200 s and an amplitude of approximately 0.2 GW; about twice the level of statistical

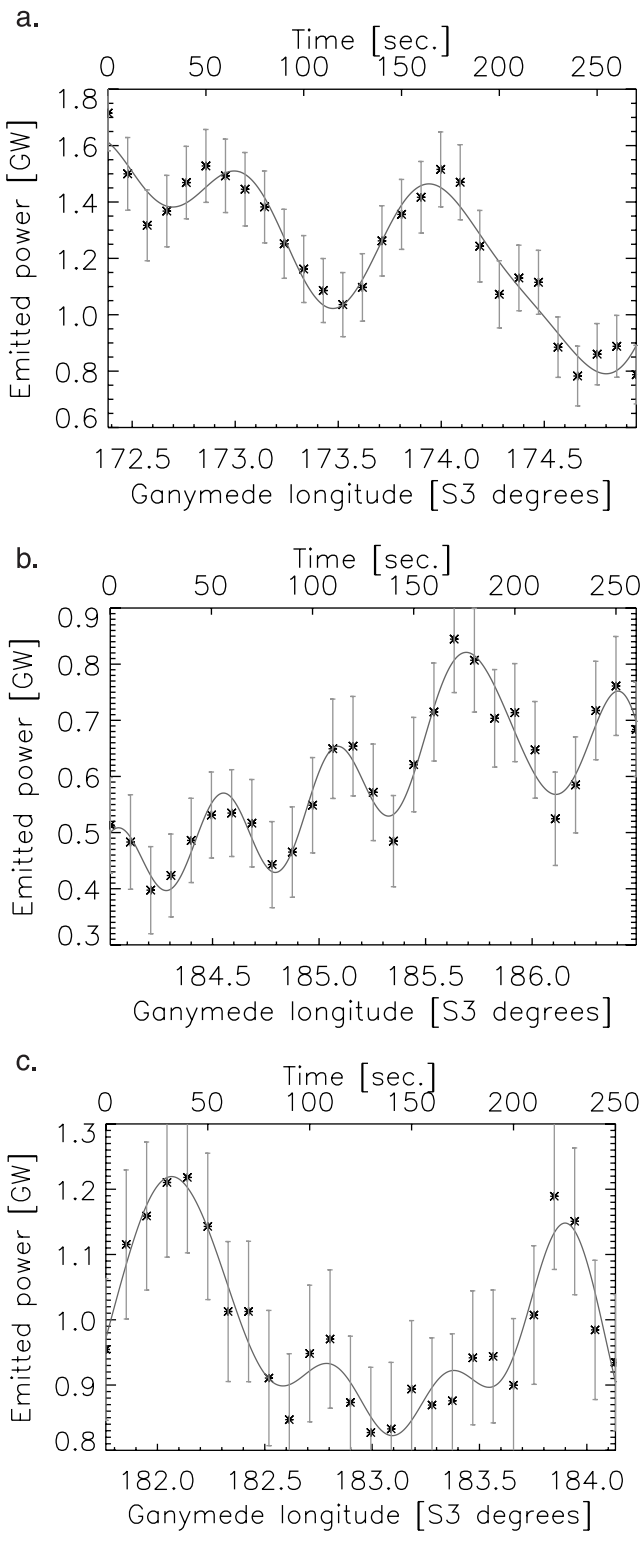

Figure 5. Illustration of the 100-s timescale. The auroral power emitted at the GFP above the BKG emission is plotted as a function of the S3 orbital longitude of Ganymede derived from HST/STIS time tagged sequences. (a) The 28 data points were determined from the 30 subimages constructed from a time-tagged sequence obtained with STIS on 26 July 1998. The solid line is obtained with a Fourier series fit with four harmonics. The error bars stand for the Poisson noise. The peak-to-peak or valley-to-valley distance is smoothly growing with Ganymede's longitude (80–130 s). (b) Same as Figure 5a; the GFP power variations were observed on 18 December 2000. Five peaks clearly emerge; their distance grows almost linearly from 51.6 to 74.7 s, leading to a period growth rate of approximately 5 s every minute. (c) Other time tagged sequences show more chaotic (less periodic) variations such as on 16 December 2000 where only two peaks clearly emerge from the background. In this specific case, the interpeak distance is about 200 s.

fluctuations. This variability is apparent in the majority of the cases that we have considered. The time period appears to range from 100 to 500 s. However, the sampling rate changes from case to case; from one 30 s image every 70 s (owing to readout time limitations) to consecutive 150 s images, and we may not be able to discriminate the fundamental frequency from its harmonics.

[15] This restriction does not apply to the 7 STIS time-tagged sequences which we assemble in 10 s subimages. The total duration of one sequence is usually 300 s, giving rise to 30 consecutive subimages per sequence. Figure 5a displays the GFP emitted power as a function of Ganymede's orbital longitude. The 28 data points were determined from the 30 subimages constructed from a time-tagged sequence obtained with STIS on 26 July 1998. The solid line is obtained with a Fourier series fit with 4 harmonics. As for the previous plots, the error bars represent the Poisson noise. They are still significantly smaller than the power variation and clearly intercept the fitting curve. The apparent period of the oscillations is about 100 s. However, closer inspection reveals that the peak-to-peak period smoothly grows with Ganymede's longitude; from 80 to 130 sec. A similar trend occurs in the example displayed in Figure 5b, where we similarly plot the GFP power variations observed on 18 December 2000. In this second example, five peaks clearly emerge. Their separation grows almost linearly from 51.6 to 74.7 s, leading to a period growth rate of approximately 5 s every minute. A reverse trend shows up in a sequence obtained on 2 February 2003. However, in this case the GFP is relatively weak and the error bars are slightly smaller than the variation amplitude. Therefore it is difficult to ascertain whether the period is always growing or if this trend is correlated to the S3 longitude. Furthermore, such a quasisinusoidal behavior is not marked in all STIS sequences. Other examples show more chaotic variations such as on 16 December 2000 (Figure 5c) where only two peaks clearly emerge from the background. In this specific case, the interpeak distance is about 200 s, in full agreement with the timescale deduced from the dashed curves in Figures 2a and 2b.

5. Discussion

5.1. Footprint Size and Available Power

[16] In the present work, we show that the size of the GFP mapped into the magnetosphere along the magnetic field lines is much larger than the size of Ganymede. If we account for a secondary focusing effect of the flux tube, threading the GFP, near Ganymede and produced by the addition of Ganymede's internal field then, the interaction region may be approximated by a circular section with a diameter in the range 8–20 R_G. This characteristic range encloses the Alfvén wing thickness derived by *Jia et al.* [2008] which is estimated to be ~10 to 12 R_G in the azimuthal direction and 6 to 7 R_G in the radial direction, in the case of a strong interaction near the center of the current sheet. The main conclusion that could be drawn from these analyses is that the GFP does not directly result from the interaction between the plasma and Ganymede but with its mini-magnetosphere. The size of the GFP may thus correspond to the thickness of the Alfvén wing which drives the field aligned currents between Ganymede's magnetosphere and Jupiter's ionosphere, thus confirming that these currents close not only through Ganymede's mantel and ionosphere but also through its magnetosphere and tail current sheets.

[17] The maximum amount of power generated by Ganymede in an Alfvénic interaction with the Jovian magnetospheric plasma is the voltage across the interaction region multiplied by the maximum current carried in the flux tube. According to *Clarke et al.* [2004], taking the interaction region to be Ganymede's magnetosphere implies that a potential of at least 400 kV is induced across the magnetosphere in the radial direction, away from Jupiter. *Belcher* [1987] derived a simple relation in order to estimate the maximum current in the flux tube: $I = \frac{DVB}{\mu_0 v_A}$ where D is the size of the Alfvénic interaction region, V is the potential, B is the ambient magnetic field, and v_A is the local Alfvén speed. *Kivelson et al.* [2004] provide ranges of numerical values for these parameters; with an Alfvén velocity ranging from 130 to 1700 km s^{-1}, depending on plasma density and magnetic field amplitude, and a local magnetic field value between 64 and 113 nT, the current reaches a value from D*32 kA to D*730 kA, where D is the diameter of the interaction region in R_G. In order to obtain a current of 2 MA, as derived by *Jia et al.* [2008], D needs to be 64 R_G for the lower current boundary and 3 R_G for the higher current value. Similarly, with average magnetic field and Alfvén velocity values one gets a maximum flux tube current of D*232 kA, requiring D = 7 R_G to sustain a 2 MA current. This range and average value are in agreement with the Alfvén wing thickness derived by *Jia et al.* [2008] and with our present estimate of the interaction region. It is therefore reasonable to use the current derived by *Jia et al.* [2008] in order to obtain the maximum power generated in the Alfvénic interaction. A maximum power of 400 kV × 2 × 10^6 A = 800 GW might then be available from the system. A small fraction of this power is dissipated to accelerate electrons in the Jovian ionosphere. In order to get an observed emitted power of 2 GW with a 10% efficiency for converting the injected electron energy into auroral UV emission [*Grodent et al.*, 2001], one would need to inject 20 GW at the top of the ionosphere. This suggests that only 2.5% of the available power is necessary to accelerate auroral electrons; this number may be even smaller for larger induced electric potential.

5.2. The 5-Hour Timescale

[18] In a recent study *Jia et al.* [2009] suggest that 2 MA is an upper limit to the current. Taking the Pedersen conductivity of Ganymede's ionosphere to be a finite value reduces the field aligned current to 1.2 MA for the case when Ganymede is close to Jupiter's central plasma sheet. It drops to values as low as ~0.5 MA when Ganymede is farthest from the plasma sheet (near S3 longitude 20° and 200°). If one considers the larger range of currents given in the above paragraph and an interaction region characterized by a diameter D ~ 10 R_G then Ganymede should generate a maximum power of ~100 GW to 3000 GW. Assuming that, as above, only 2.5% of that power is used to accelerate auroral electrons and that only 10% of that energy is converted into UV emission, the maximum emitted power ranges from 0.25 GW to 7.5 GW, consistent

with the range of power observed in the 5-hour modulation (0.2–1.5 GW).

[19] The 5-hour quasi periodicity of the GFP emitted power and the location of the extrema all agree with an interaction process controlled by the variations of the plasma sheet density interacting with Ganymede. These variations are induced by the tilt of the current sheet with respect to Ganymede's orbital plane, with a stronger plasma density giving rise to larger emission power. *Gérard et al.* [2006] and *Serio and Clarke* [2008] highlighted a similar evolution of the Io footprint brightness. They suggested that the long timescale brightness variations are controlled by the system III longitude of Io and its position above or below the center of the torus, with interaction strength proportional to the torus density.

5.3. The 10–40 Minute Timescale

[20] We have shown that the GFP emitted power significantly changes within 10 to 40 minutes. It is important to remember that such a variation is not systematic since about one fourth of the selected images do not display any clear temporal modulation. There are very few processes able to account for a power variation on a timescale of the order of a fraction of one hour. One of them accounts for observations of the Jovian plasma with Galileo's energetic particles detector (EPD) which suggest that the plasma is constantly changing. Long term angle-averaged energy spectrograms of electrons and ions all the time show measurable variations at timescales less than an hour. Among this variability, *Mauk et al.* [1999] highlighted plasma injection events characterized by dispersion of energy with time. They analyzed over 100 injection events, showing a clear energy dispersion signature, spanning ~1 year of observation with Galileo/EPD. The characteristic timescale for these injections (i.e. the time during which they leave a measurable signature in the detector) is commonly less than an hour and can be as short as 10 minutes. They occur at all S3 longitudes and show no preferred local time position. They were observed everywhere between 9 and 27 R_J, with a peak near 11–12 R_J. Even during quiet periods, when no energy-time dispersed events are reported, modest transient features are observed with timescales much less than 5 hours. Galileo measurements have shown evidence of energetic electron injections interacting with Ganymede's magnetosphere [*Williams et al.*, 1997]. Even though these observations were not further established by statistical reoccurrence, they strongly suggest that short timescale (of a fraction of an hour) energetic dynamics influence Ganymede's magnetospheric environment. We should insist that the occurrence of injection events is just one mechanism that we consider to be reasonably possible source of auroral variability. Inside Ganymede's magnetosphere, the convection time highly depends on the ionospheric conductivity. Galileo EPD estimates show an upper limit to the plasma flow of 25–45 km s^{-1} in the polar cap [*Williams et al.*, 1997]. Accordingly, convection time of the open flux from upstream to downstream across the magnetospheric region, taken to be 10 R_G, should be on the order of 10 to 20 minutes, close to the expected range. However, this similarity is not sufficient to establish the role of convection in the 10–40 minutes variability, since it does not explain by itself the recurrence of the auroral variation.

5.4. The 100-s Timescale

[21] At least two different mechanisms could trigger the shortest timescale periodicity and one does not necessarily exclude the other. The 100 s timescale is very close to the quasiperiodic occurrence of flux transfer like events (FTEs) associated with bursty reconnection on Ganymede's magnetopause. These rapid events have been observed in the Galileo MAG data and in the MHD simulations of *Jia et al.* [2008]. Their periodicity varies from 20 to 40 sec., depending on the local plasma conditions, and may modulate the field-aligned currents accordingly and thus the GFP emission power. On the other hand, *Bonfond et al.* [2007] found brightness variability for the different components of the Io footprint with similar timescales as for Ganymede. The authors notably highlight cases of simultaneous variations of the main and the secondary spot in the southern hemisphere. They claim that correlated fluctuations of the spots brightness cannot be attributed to local perturbations at Io but should be linked to the acceleration or precipitation regions. Furthermore, S-burst radio emissions recently analyzed by *Hess et al.* [2009] show quasiperiodic occurrences of ~1 kV potential drops with timescales of ~200 s. These acceleration structures then appear to drift away from the planet and to disappear after ten minutes. Consequently, another scenario would be that the short timescale fluctuations of Ganymede's footprint could be caused by the same mechanism as for Io: repeated occurrence of acceleration structures located approximately 1 R_J above the Jovian surface.

6. Summary

[22] Ganymede has a privileged rank in Jupiter's realm. Galileo in situ observations have revealed that it is the sole Galilean satellite having an internal magnetic field strong enough to carve its own minimagnetosphere inside Jupiter's. The perturbation caused by the incessant collision of Jupiter's magnetospheric fast flowing plasma with Ganymede's magnetosphere propagates along Jupiter's magnetic field lines and forms two Alfvén wings. They carry field aligned currents from and down to Jupiter's northern and southern ionosphere where they produce the measurable auroral footprint of Ganymede.

[23] We analyzed 753 FUV images obtained with HST from 2000 to 2008, showing the footprint of Ganymede wandering among the other components of Jupiter's complex aurora. The size of the auroral footprint is much larger than Ganymede's cross-section projected on the Jovian surface along the magnetic field lines. It maps to a circular region in the equatorial plane with a characteristic diameter of 8 to 20 R_G. This range is in agreement with the values derived from a three-dimensional MHD model simulating the interaction between the Jovian plasma and Ganymede's magnetosphere. The size of the GFP may thus correspond to the thickness of the Alfvén wing which drives the field aligned currents between Ganymede's magnetosphere and Jupiter's ionosphere. Therefore it strongly suggests that these currents are closing through Ganymede and its ionosphere as well as through its magnetosphere and tail current sheets.

[24] The short exposure times (a few tens of s) and the availability of time tagged images allowed us to perform an

in depth temporal analysis of the auroral power emitted at the footprint of Ganymede. Three timescales emerge from this study: 5 hours, 10 to 40 minutes, and 100 s.

[25] 1. The 5-hour timescale appears to be periodic and associated with the periodic flapping of the tilted Jovian plasma sheet over Ganymede. This movement changes the plasma density interacting with Ganymede and modulates the interaction strength and the auroral power emitted by the GFP with S3 longitude. The magnitude of the emitted power inferred from HST images ranges from 0.2 GW to 1.5 GW, corresponding to an injected power of 2 to 15 GW. These numbers are in agreement with the 0.25 to 7.5 GW range, based on the estimated maximum power generated in the Alfvénic interaction of Ganymede with the Jovian plasma.

[26] 2. The 10–40 minute timescale refers to auroral power variations with amplitude of ~1 GW which are observed in 64% of the data set. Since this timescale is comparable to the available portion of one HST orbit, we cannot verify if the modulation is periodic or simply recurrent. Few processes are able to account for this variability. Galileo observations of energetic particles between 9 and 27 R_J revealed energetic events, such as plasma injections, which could locally increase the interaction strength with Ganymede. The characteristic time of these events is commonly less than an hour and may be as short as 10 minutes.

[27] 3. The 100-s timescale is found in almost all image sequences. However, it can only be firmly established for the time tagged images where these fluctuations of Ganymede's auroral emission are quasiperiodic. The amplitude is relatively small, ~0.2 GW, but it is twice larger than the statistical fluctuations. The cases that we have studied show an apparent period which is either increasing or decreasing linearly during the ~5 minutes exposures. These very short variations appear to be reminiscent of the quasiperiodic occurrence of FTEs associated with bursty reconnection on Ganymede's magnetopause, observed with Galileo and simulated with an MHD model. On the other hand, similar brightness variations of the auroral footprint of Io have been interpreted in terms of processes taking place far from the satellite; in the acceleration or precipitation region above the atmosphere of Jupiter, as suggested by the presence of acceleration structures whose S-burst radio signature reoccurs every ~200 s.

[28] These three levels of GFP emitted power variations are taking place simultaneously. They give rise to the apparently complex distribution shown in Figure 3. Further observations and data processing will be necessary to extend this analysis to the fainter auroral footprint of Europa. The above results provide original constraints on the interaction between Ganymede and Jupiter, and more generally between moving plasma and a magnetized body.

[29] **Acknowledgments.** The authors would like to thank Margaret Kivelson at UCLA for helpful discussions and two anonymous reviewers who provided constructive comments and suggestions. This work is based on observations with the NASA/ESA Hubble Space Telescope, obtained at the Space Telescope Science Institute (STScI), which is operated by AURA, Inc., for NASA under contract NAS5-26555. D.G., B.B., J.C.G., and A.R. are supported by the Belgian Fund for Scientific Research (FNRS) and the PRODEX Program managed by the European Space Agency in collaboration with the Belgian Federal Science Policy Office. X.J. is supported by NASA under grants NNG05GB82G and NNX08AQ46G. J.D.N. is supported by STFC grant PP/E000983/. Work in Boston was supported by grants HST-GO-10862.01-A and HST-GO-10507.01-A from the Space Telescope Science Institute to Boston University.

[30] Wolfgang Baumjohann thanks Emma Bunce and another reviewer for their assistance in evaluating this paper.

References

Belcher, J. W. (1987), The Jupiter-Io connection: An Alfvén engine in space, *Science*, *238*, 170–176.

Bonfond, B., J.-C. Gérard, D. Grodent, and J. Saur (2007), Ultraviolet Io footprint short timescale dynamics, *Geophys. Res. Lett.*, *34*, L06201, doi:10.1029/2006GL028765.

Bonfond, B., D. Grodent, J.-C. Gérard, A. Radioti, J. Saur, and S. Jacobsen (2008), UV Io footprint leading spot: A key feature for understanding the UV Io footprint multiplicity?, *Geophys. Res. Lett.*, *35*, L05107, doi:10.1029/2007GL032418.

Bonfond, B., D. Grodent, J.-C. Gérard, A. Radioti, V. Dols, P. Delamere, and J. T. Clarke (2009), The Io footprint UV tail: Location, altitude and vertical distribution, *J. Geophys. Res.*, doi:10.1029/2009JA014312, in press.

Bunce, E. J., P. G. Hanlon, and S. W. H. Cowley (2002), A simple empirical model of the equatorial radial field in Jupiter's middle magnetosphere, based on spacecraft fly-by and Galileo orbiter data, *Planet. Space Sci.*, *50*, 789–806.

Clarke, J. T., et al. (2002), Ultraviolet auroral emissions from the magnetic footprints of Io, Ganymede, and Europa on Jupiter, *Nature*, *415*, 997–1000.

Clarke, J. T., D. Grodent, S. Cowley, E. Bunce, P. Zarka, J. Connerney, and T. Satoh (2004), Jupiter's aurora, in *Jupiter: The Planet, Satellites and Magnetosphere*, edited by F. Bagenal, B. McKinnon, and T. Dowling, pp. 639–670, Cambridge Univ. Press, New York.

Feldman, P. D., M. A. McGrath, D. F. Strobel, H. W. Moos, K. D. Retherford, and B. C. Wolven (2000), HST/STIS ultraviolet imaging of polar aurora on Ganymede, *Astrophys. J.*, *535*, 1085–1090, doi:10.1086/30889.

Gérard, J.-C., A. Saglam, D. Grodent, and J. T. Clarke (2006), Morphology of the ultraviolet Io footprint emission and its control by Io's location, *J. Geophys. Res.*, *111*, A04202, doi:10.1029/2005JA011327.

Grodent, D., J. H. Waite Jr., and J.-C. Gérard (2001), A self-consistent model of the Jovian auroral thermal structure, *J. Geophys. Res.*, *106*(A7), 12,933–12,952.

Grodent, D., J. T. Clarke, J. H. Waite, J. Kim, and S. W. H. Cowley (2003a), Jupiter's main auroral oval observed with HST-STIS, *J. Geophys. Res.*, *108*(A11), 1389, doi:10.1029/2003JA009921.

Grodent, D., J. T. Clarke, J. H. Waite Jr., S. W. H. Cowley, J.-C. Gérard, and J. Kim (2003b), Jupiter's polar auroral emissions, *J. Geophys. Res.*, *108*(A10), 1366, doi:10.1029/2003JA010017.

Grodent, D., B. Bonfond, J.-C. Gérard, A. Radioti, J. Gustin, J. T. Clarke, J. Nichols, and J. E. P. Connerney (2008a), Auroral evidence of a localized magnetic anomaly in Jupiter's northern hemisphere, *J. Geophys. Res.*, *113*, A09201, doi:10.1029/2008JA013185.

Grodent, D., J.-C. Gérard, A. Radioti, B. Bonfond, and A. Saglam (2008b), Jupiter's changing auroral location, *J. Geophys. Res.*, *113*, A01206, doi:10.1029/2007JA012601.

Hess, S., P. Zarka, F. Mottez, and V. B. Ryabov (2009), Electric potential jumps in the Io-Jupiter flux tube, *Planet. Space Sci.*, *57*, 23–33, doi:10.1016/j.pss.2008.10.006.

Jia, X., R. J. Walker, M. G. Kivelson, K. K. Khurana, and J. A. Linker (2008), Three-dimensional MHD simulations of Ganymede's magnetosphere, *J. Geophys. Res.*, *113*, A06212, doi:10.1029/2007JA012748.

Jia, X., R. J. Walker, M. G. Kivelson, K. K. Khurana, and J. A. Linker (2009), Properties of Ganymede's magnetosphere inferred from improved three-dimensional MHD simulations, *J. Geophys. Res.*, doi:10.1029/2009JA014375, in press.

Khurana, K. K. (2001), Influence of solar wind on Jupiter's magnetosphere deduced from currents in the equatorial plane, *J. Geophys. Res.*, *106*(A11), 25,999–26,016.

Khurana, K. K., and H. K. Schwarzl (2005), Global structure of Jupiter's magnetospheric current sheet, *J. Geophys. Res.*, *110*, A07227, doi:10.1029/2004JA010757.

Khurana, K. K., M. G. Kivelson, V. M. Vasyliunas, N. Krupp, J. Woch, A. Lagg, B. H. Mauk, and W. S. Kurth (2004), The configuration of Jupiter's magnetosphere, in *Jupiter: The Planet, Satellites and Magnetosphere*, edited by F. Bagenal, B. McKinnon, and T. Dowling, pp. 593–616, Cambridge Univ. Press, New York.

Kivelson, M. G., K. K. Khurana, C. T. Russell, R. J. Walker, J. Warnecke, F. V. Coroniti, C. Polanskey, D. J. Southwood, and G. Schubert (1996), Discovery of Ganymede's magnetic field by the Galileo spacecraft, *Nature*, *384*, 537–541.

Kivelson, M. G., F. Bagenal, W. S. Kurth, F. M. Neubauer, C. Parnaicas, and J. Saur (2004), Magnetospheric interactions with satellites, in

Jupiter: The Planet, Satellites and Magnetosphere, edited by F. Bagenal, B. McKinnon, and T. Dowling, pp. 513–536, Cambridge Univ. Press, New York.

Mauk, B. H., D. J. Williams, R. W. McEntire, K. K. Khurana, and J. G. Roeder (1999), Storm-like dynamics of Jupiter's inner and middle magnetosphere, *J. Geophys. Res.*, *104*(A10), 22,759–22,778.

Nichols, J. D., J. T. Clarke, J. C. Gérard, D. Grodent, and K. C. Hansen (2009), The variation of different components of Jupiter's auroral emission, *J. Geophys. Res.*, doi:10.1029/2009JA014051, in press.

Radioti, A., A. T. Tomàs, D. Grodent, J.-C. Gérard, J. Gustin, B. Bonfond, N. Krupp, J. Woch, and J. D. Menietti (2009), Equatorward diffuse auroral emissions at Jupiter: Simultaneous HST and Galileo observations, *Geophys. Res. Lett.*, *36*, L07101, doi:10.1029/2009GL037857.

Serio, A. W., and J. T. Clarke (2008), The variation of Io's auroral footprint brightness with the location of Io in the plasma torus, *Icarus*, *197*, 368–374.

Williams, D. J. (2004), Energetic electron beams in Ganymede's magnetosphere, *J. Geophys. Res.*, *109*, A09211, doi:10.1029/2004JA010521.

Williams, D. J., B. Mauk, and R. W. McEntire (1997), Trapped electrons in Ganymede's magnetic field, *Geophys. Res. Lett.*, *24*(23), 2953–2956.

B. Bonfond, J.-C. Gérard, D. Grodent, and A. Radioti, Institut d'Astrophysique et de Géophysique, Laboratory for Planetary and Atmospheric Physics, Université de Liège, Allée du 6 Août, 17 (B5c), B-4000 Liège, Belgium. (d.grodent@ulg.ac.be)

J. T. Clarke, Center for Space Physics, Boston University, 725 Commonwealth Avenue, Boston, MA 02215, USA.

X. Jia, Institute of Geophysics and Planetary Physics, University of California, Box 951567, Los Angeles, CA 90095, USA.

J. D. Nichols, Department of Physics and Astronomy, University of Leicester, Leicester LE1 7RH, UK.